SF2A 2011
G. Alecian, K. Belkacem, R. Samadi and D. Valls-Gabaud (eds)

BULGE FORMATION PATTERNS IN AP^{3}M-SPH SIMULATIONS: QUESTIONS TO BE ANSWERED BY FUTURE MISSIONS

A. Obreja[1], R. Domínguez-Tenreiro[1], M. Doménech-Moral[2], F. J. Martínez-Serrano[2] and A. Serna[2]

Abstract. The few observations of bulges available suggest a bi-modality in their properties, feature we have also found in high resolution hydrodynamical simulations in a cosmological context. The latter gives important information about bulge formation processes, facilitating the comparison with available observational data, as well as serving as guideline for future observational strategies. We conclude that in this particular field, there is much need for more in depth observations of large samples in order to distinguish among the variety of possible bulge formations paths.

Keywords: theory, galaxies, bulges, structure, kinematics, abundances

1 Introduction

It has been a long-standing matter of debate whether elliptical galaxies (Es from now on) and classical bulges of spirals (see bulge classification in Kormendy & Kennicutt 2004) share a similar formation history, since they have in common at least part of their observed properties. For example, both types of objects seem to share the same fundamental plane, their rotational support correlates with their shape in a similar manner, and both are α-element enhanced.

Concerning observational studies of spiral galaxies in particular, stellar population studies of external bulges, as well as of the Milky Way Bulge, showed that many classical bulges appear as an older and kinematically hotter population superimposed on a secondary, younger one with kinematics more similar to disks, in resemblance with the blue cores found in some Es. Also, the two populations have different metallicities and α-element enhancements, their mixing leading to a wide range of observed abundance gradients.

In the case of Es, analytical models as well as N-body simulations revealed that the halo mass assembly process follows a two-phase scenario, with a first violent one characterized by high mass aggregation rates and resulting from collapse-like and merger events, and a latter one with lower mass aggregation rates (Wechsler et al. 2002; Zhao et al. 2003). This scenario was confirmed later on in hydrodynamical simulations (Domínguez-Tenreiro et al. 2006, 2011; Oser et al. 2010).

In this frame, our objective is to test whether this two-phase formation scenario, proposed for Es, could also explain the up-to-now observations of classical bulges. Therefore, we want to know if it can account for the characteristics of bulge observations, like the duality in stellar populations (Ellis et al. 2001; Thomas & Davies 2006; Carollo et al. 2007), the variety of age and metallicities gradients (MacArthur et al. 2009; Sánchez-Blázquez et al. 2011), or some secular-like morphologies (Prugniel et al. 2001; Peletier et al. 2007).

2 Theoretical Approach to Bulge Formation

Bulge formation has been linked to apparently diverging processes like hierarchical structure formation and monolithic collapse, or to secular instabilities of the galactic disks. However, not one such process alone can explain the diversity of bulge shapes, sizes, abundances, kinematics and profiles observed, although these observations are still scarce. For this reason, hydrodynamical simulations in a cosmological context are a powerful

[1] Departamento de Física Teórica, Universidad Autónoma de Madrid, 28049 Cantoblanco, Madrid, Spain
[2] Departamento de Física y Arquitectura de Computadores, Universidad Miguel Hernández, 032202 Elche, Alicante, Spain

tool to disentangle the variety o possible paths leading to bulge formation. Progress in this topic requires increasing the observational data on bulges, not only in number but in spacial and spectral resolution as well.

The simulations we have analyzed have been performed using an OpenMP parallel version of the DEVA code (Serna et al. 2003), in which special emphasis was put on conservation laws. The chemical feedback and cooling methods have been described in Martínez-Serrano et al. (2008). In brief, the statistically implemented chemical evolution accounts for the full dependence of metal production on the detailed composition of the stellar particles, the metals diffusing among gas particles. A probabilistic approach for the delayed gas restitution from stars reduces the statistical noise, allowing the study of the chemical structure of small scale structures –like bulges– at an affordable computational cost.

Low-resolution simulations that consisted of different Monte Carlo realizations of the same cosmological model: a flat ΛCDM (with $\Omega_\Lambda = 0.723$, $\Omega_m = 0.277$, $\Omega_b = 0.04$, and $h = 0.7$) within a periodic box of 10 Mpc per side were performed (Doménech-Moral et al. 2011). Afterwards, massive gas-rich objects with a prominent gas disk at $z = 0$ were selected from high (HD) and low density (LD) regions, and resimulated at high resolution. The baryonic mass of these galaxies is of the order of 10^{10} $M_\odot$, with a mass resolution of $\sim 10^5$ (baryons) and 10^6 $M_\odot$ (DM), respectively. The minimum SPH smoothing length is 0.2 h^{-1} kpc, while the star formation (SF) follows a Kennincutt–Schmidt-like law with an efficiency ≤ 0.01 and a density threshold $\sim 10^{-25}$ g cm^{-3}.

Doménech-Moral et al. (2011) analyzed the disk galaxies simulated as described above from the point of view of their fine structure. They identified different components (thin and thick disc, halo, bulge) with properties in good consistency with observations, in particular bimodal bulge metalicities and [α/Fe] distributions, that they interpret as resulting from fast and slow modes of SF. In our work, we study in detail the intrinsic properties of these simulated (classical) bulges, specifically focusing on the mass-averaged three-dimensional sizes, shapes and kinematics, as well as their stellar ages and abundances, in connection with their formation history.

3 Bulge Formation Patterns

In order to see how bulges actually get assembled, we looked at the snapshots of the simulated objects between a redshift of ~ 9 to the present epoch. In this manner, we were able to identify the two mass aggregation modes which were also found in simulations of Es. Thus, we noticed a first fast collapse phase with high mass aggregation rates and violent episodes of star formation, and a secondary quieter mode in which gas is more continuously accreted on the central, already formed, old, stellar spheroid, being slowly transformed into stars. Given this behavior, we look for a criteria which we could use to separate the bulge stars formed in these two phases, and therefore constructed the star formation rate histories (SFRHs) and the mass assembly tracks (MATs) of the simulated objects. An example of such a plot for a particular object is given in the left panel of Fig. 2, where we can observe a correlation between the dark matter halo major mergers and the peaks in the star formation rate at the bulge scale, the latter appearing as a delayed consequence of the former. Also, the MAT jumps at the galaxy (dashed cyan lines) and virial radius (solid black line) scales are correlated with those at the bulge scale (solid red, green, blue, magenta and orange lines), therefore reinforcing the importance of cosmological gas inflow on bulge formation. Therefore, we separated the old from the young stellar bulge at $z = 0$ based on the point where the SFR tail begins, point also correlated with the beginning of the slowly increasing plateau in the MAT at the bulge scale, exemplified in the figure by the vertical dashed line.

We should mention that for objects in high density environments, the slow phase of bulge assembly can show imprints of major mergers with associated starbursts. In these cases, we considered the bulge stars forming during these SFR maxima as a distinct component, which we dubbed "intermediate".

In order to exemplify the two modes of bulge formation, we constructed Fig. 1, in which we give a redshift sequence of a particular projection in position of an object from a low-density region, LD-5101A. Basically, the two left-most panels correspond to redshifts from the fast phase, while the two right-most ones to zs from the slow mode. In this case, the temporal separation between the old (red) and the young one (blue) stellar population is $z \sim 2.1$ and roughly corresponds to the center-right snapshot. The center-left panel also corresponds to an important point in the bulge evolution, at this redshift the SFR attaining its highest value. In this snapshot we see the old bulge condensed at the densest points of the flow converging regions, while the young bulge-to-be stars are still found as gaseous particles spanning a much wider volume. These different aggregation modes of the old and young bulge can be distinguished, however, from much earlier on (see left panel in the same figure).

Even before the beginning of the slow mode, the old bulge in in place as a spheroid, the gas which will come to form the young bulge stars appearing as a disk-like structure centered on this spheroid. This behavior can be seen in the center-right panel of Fig. 1. The $z = 1.14$ snapshot depicts a stage in which the young bulge is

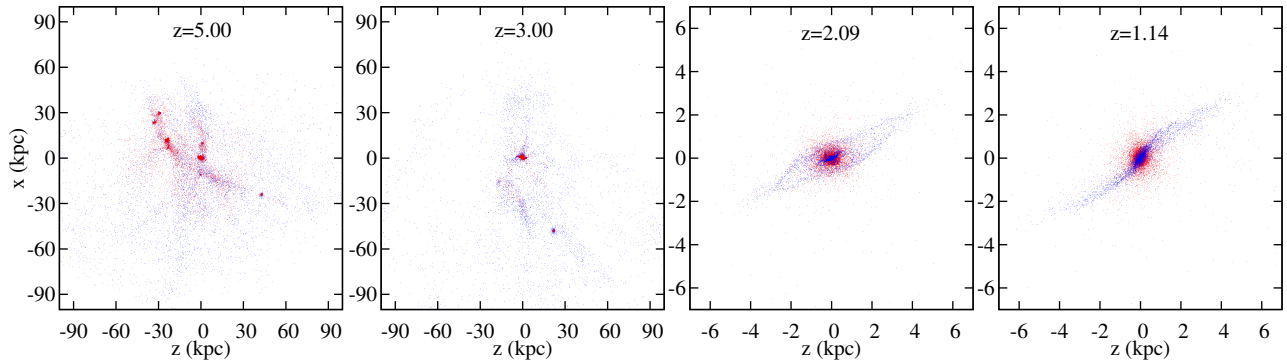

Fig. 1. Position projections of old (red) and young (blue) bulge-to-be stellar particles at $z = 0$ at four different redshifts for object LD-5101A.

still clearly structured as a disk, this particular redshift corresponding to the moment when approximately half of the young bulge is already found as stellar particles, By redshift 0, all these particles will be found as stars within a sphere of 1.85 kpc (for LD-5101A), the young bulge still "remembering" its distinct formation pattern.

These bulge assembly patterns resemble the two phases found by Domínguez-Tenreiro et al. (2006, 2011) for more massive spheroids, the main difference being the fact that, in the case of massive ellipticals almost all the gas is transformed into stars at the flow converging regions along the first phase, while no such exhaustive gas consumptions occurs for bulges.

4 Properties of Simulated Bulges

In the simulated bulges, the sizes, shapes, kinematics, stellar ages and metal contents of the stellar populations formed in these distinct phases can be well distinguished. In this respect, we found the youngest component to be more centrally concentrated, with disk-like morphology, more rotationally supported, with roughly solar metallicities and sub-solar α-element enhancements. The oldest population, in contrast, is more spheroid-like, has clearly sub-solar metallicities and larger α-element enhancements.

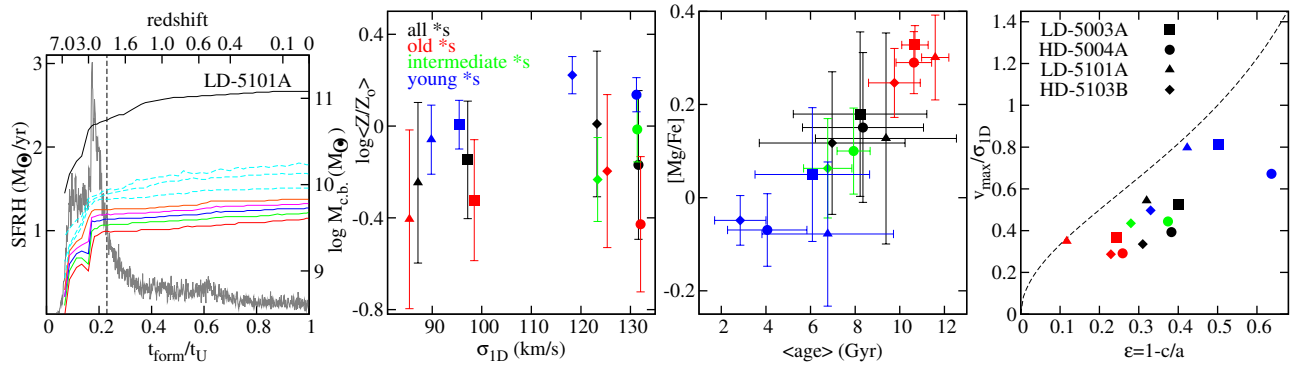

Fig. 2. Left: SFRH of bulge HD-5101A (grey line) superimposed on the temporal evolution of cold gas plus stellar mass inside fix radii (solid black for total mass inside the virial radius, dashed cyan for radii exceeding r_{bulge}, and solid red, green, blue, magenta and orange for radii roughly within r_{bulge} with the radius increasing from bottom to top); the vertical black dashed line marks the separation between the old and the young bulges. **Center-left:** average metallicity vs. 1D velocity dispersion. **Center-right:** [Mg/Fe] vs. average age. **Right:** Rotational support vs. shape parameter.

These findings are exemplified in Fig. 2, where we give some of the global properties of both bulges as well as their distinct stellar components at redshift 0. The center-left panel for e.g. shows the average metallicity versus the 1D velocity dispersion, in which a clear trend can be noted, Z increasing with σ_{1D} (more rapidly for the younger components), as well as with the age.

Additionally, the center-right panel gives the [Mg/Fe] as a tracer of α-enhancement versus average stellar

age, in which is obvious that the α-enhancement is an age effect, the youngest a population the lower its average [Mg/Fe]. The right-most panel comes to sustain our argument that the younger bulge is more rotationally supported and more oblate than the old one. The shape parameter, ε in this case, was computed from the principal axis lengths of the inertia tensor. In this last panel, we can see that all four bulges, as well as their different components appear below the curve of oblate spheroids flattened only by rotation (dashed black curve), the shape parameter together with the amount of rotational support increasing with the average stellar age.

These global properties predicted by simulations can be used to design effective observational strategies for bulges, in order to take advantage of the ever more powerful instruments both on Earth as well as in space, easing in this manner the cumbersome task of comparing observations with theoretical predictions.

5 Conclusions

We find our sample bulges to have a mass-dominant old stellar population, formed at high z in a fast collapse-like event, and one or two younger populations formed later on, during a second phase generally characterized by lower mass assembly and SF rates. The bulge stars resulting from the fast mode form an object with properties similar to low mass spheroids, while those which are a consequence of the later slow mode show global characteristics more typical of disks. The variety of processes which can act during the second phase (minor and major mergers, disk secular instabilities, satellite incorporation) together with continuous gas accretion result in objects with different characteristics, that fit well with the important dispersion in bulge properties observationally found. We also noticed correlations between the evolution of the DM halo and the SFR at the bulge scale, reinforcing the importance of cosmologically driven processes in bulge formation. These results are not only important for testing the physical conditions necessary for bulges formation, but also as guidelines for observational strategy designs, field in which there is room for ample improvements.

From an observational perspective although much progress has been made with surveys like SAURON, there still remain some important questions regarding bulge formation and evolution mechanisms. Some of them are related to the role of major mergers in galaxy evolution or to the process of satellite cannibalism. Equally important are also the bars, for e.g. their frequency with redshift and their life cycle. In this latter issue, a better understanding of the intrinsic properties of pseudobulges would provide much insight into the bulge classification schemes. On the other hand, although we have today the hierarchical structure formation paradigm, the details of cold gas inflows, an important mechanism in bulge formation, are not yet fully understood. Least but not last, bulges are thought to evolve in some sort of correlation with the massive black holes they host, problem which is still far from being successfully tackled.

Solving these problems requires high resolution spatial and spectroscopic surveys, extended in redshift as much as possible. In this respect, the HST's survey mission CANDELS, the Wide-field Infrared Survey Explorer (WISE), or the Next Generation Virgo cluster Survey (NGVS) at CFHT will add important observational data to that provided up to now by telescopes like Spitzer, Hershel, WHT or Gemini-North.

References

Carollo, C. M., Scarlata, C., Stiavelli, M., Wyse, R. F. G., & Mayer, L. 2007, ApJ, 658, 960
Doménech-Moral, M., Martínez-Serrano, F., Domínguez-Tenreiro, R., & Serna, A. 2011, MNRAS, submitted
Domínguez-Tenreiro, R., Oñorbe, J., Martínez-Serrano, F., & Serna, A. 2011, MNRAS, 413, 3022
Domínguez-Tenreiro, R., Oñorbe, J., Sáiz, A., Artal, H., & Serna, A. 2006, ApJ, 636, 77
Ellis, R. S., Abraham, R. G., & Dickinson, M. 2001, ApJ, 551, 111
Kormendy, J. & Kennicutt, Jr., R. C. 2004, ARA&A, 42, 603
MacArthur, L. A., González, J. J., & Courteau, S. 2009, MNRAS, 395, 28
Martínez-Serrano, F. J., Serna, A., Domínguez-Tenreiro, R., & Mollá, M. 2008, MNRAS, 388, 39
Oser, L., Ostriker, J. P., Naab, T., Johansson, P. H., & Burkert, A. 2010, ApJ, 725, 2312
Peletier, R. F., Falcón-Barroso, J., Bacon, R., et al. 2007, MNRAS, 379, 445
Prugniel, P., Maubon, G., & Simien, F. 2001, A&A, 366, 68
Sánchez-Blázquez, P., Ocvirk, P., Gibson, B. K., Pérez, I., & Peletier, R. F. 2011, MNRAS, 415, 709
Serna, A., Domínguez-Tenreiro, R., & Sáiz, A. 2003, ApJ, 597, 878
Thomas, D. & Davies, R. L. 2006, MNRAS, 366, 510
Wechsler, R. H., Bullock, J. S., Primack, J. R., Kravtsov, A. V., & Dekel, A. 2002, ApJ, 568, 52
Zhao, D. H., Mo, H. J., Jing, Y. P., & Börner, G. 2003, MNRAS, 339, 12